Cleavage modelling with experimental particle size distribution and novel particle failure criterion

Andrey P Jivkov[1,*], **Peter James**[2]

[1] School of Mechanical, Aerospace and Civil Engineering, The University of Manchester, Manchester M13 9PL, UK.
[2] AMEC, Walton House, Birchwood, Warrington WA3 6GN, UK.
* Corresponding author: andrey.jivkov@manchester.ac.uk

Abstract Most of the existing local approaches for cleavage fracture derive from the assumptions that global failure is a weakest-link event and that only the tail of the size distribution of micro-crack initiating features is significant. This appears to be sufficient in predicting lower shelf toughness under high constraint conditions, but may fail when attempting to predict toughness in the transition region or for low constraint conditions when using the same parameters. While coupled ductile damage models with Beremin-like failure probability could be useful in the transition region, uncoupled models with "a posteriori" probability calculations are advantageous to the engineering community. Cleavage toughness predictions in the transition regime, which can be extended to low constraint conditions, are here made with improved criterion for particle failure and experimentally based size distribution of initiators for specific RPV steel. The model is shown to predict experimentally measured locations of cleavage initiators. Further, the model predicts the fracture toughness in a large part of the transition region and accurately predicts a measured shift with irradiation. All results are obtained without changes in model parameters. This suggests that the model can be used for assessing toughness changes due to constraint- and temperature-driven plasticity changes.

Keywords RPV steel; local failure criterion; global failure probability; transition temperature regime

1. Introduction

Safety assessment and life extension decisions in nuclear plant require reliable methodologies for predicting changes in cleavage fracture toughness behaviour of ferritic RPV steels due to irradiation and defect geometry effects. Local approaches (LA) to cleavage fracture are promising as these could account for the micro-mechanisms involved in the cleavage failure phenomenon, such as the nucleation of micro-cracks at second-phase brittle particles, the propagation of such micro-cracks within grains and the propagation of a critical micro-crack leading to component failure [1]. The pioneering LA to cleavage, proposed by the Beremin group [2], is based on two main assumptions: that the global failure probability is a weakest-link event and that the individual failure probabilities are dictated by local mechanical fields and specific microstructure data such as the size distribution and number density of cleavage-initiating particles. Assuming that the tail of the size distribution can be approximated by a power-law, the weakest-link statistics leads to a global failure probability expressed as a Weibull-type function of a generalised stress, the Weibull stress σ_w [2, 3]:

$$P_f(V) = 1 - \exp\left[-\left(\frac{\sigma_w}{\sigma_u} \right)^m \right] \tag{1}$$

The shape, m, and scale, σ_u, of the Weibull function can be calibrated using fracture toughness data obtained with particular crack geometry at a given temperature and corresponding FE analysis [4]. For calibrations performed with high-constraint crack geometries at or below the ductile-to-brittle transition temperature, T_0, the shape and scale obtained can be used with sufficiently good accuracy to predict cleavage fracture toughness of other high-constraint geometries at temperatures below T_0 [2-4]. However, an attempt to use the same parameters to calculate cleavage toughness under lower constraint conditions or higher temperatures leads to predictions that do not match experimental values. For cleavage fracture toughness data obtained at a given temperature with low- and high-constraint geometries, independent calibrations would typically show that the low-constraint m

is smaller than the high-constraint m (assuming that σ_u is not dependent on constraint), see e.g. [5]. This suggests that the excess of plastic deformations introduced by the lower constraint require reduction of m to make reliable predictions. The methodology proposed in [5] for cross-calibration of m between high and low constraint geometries has shown promise [5, 6], but remains limited to temperatures well below T_0, where the lower constraint conditions do not introduce substantial increase in plastic deformations relative to the high constraint case. This may prove problematic when used to predict cleavage fracture toughness for short cracks in irradiated material, where the reference temperature is shifted to higher values. To predict the irradiation effects on cleavage one needs a reliable model for the ductile-to-brittle transition (DBT) regime. Here, however, the Weibull parameters need to be varied to match experimental data. One possibility is to keep the shape parameter constant, which leads to temperature dependence of the scale, σ_u [7, 8]. Another possibility is to keep the scale parameter constant, which leads to temperature dependence of the shape, m [9, 10]. As for the low-constraint situation, m needs to be reduced with increasing temperature, i.e. with enhanced plasticity.

Considering the physical basis for the Beremin LA [2, 3], the current state of affairs is not satisfactory, because the Weibull parameters must depend exclusively on the material microstructure. If the model for individual failure probability accounted adequately for the local fields and microstructure effects on particle failure, and the global failure were a weakest-link event, then the changes in plasticity due to constraint reduction or temperature increase should be already accounted for, leaving the Weibull parameters constants. In particular, m should be linked to the shape of size distribution of cleavage initiation particles, while σ_u should depend on the elastic properties and surface energy of the material as well as on the scale of the particle size distribution. Since these parameters do not change noticeably with constraint or temperature, the need to vary m and σ_u at increasing plastic deformations suggests that the link between physics and mechanics breaks. One possibility is that the individual failure probability model does not account adequately for the mechanical and particle size effects. A second possibility is that with the increase of plastic deformations the population of micro-cracks that needs to be accounted for in the weakest-link statistics becomes larger than the tail of the distribution, approximated by power-law in the Weibull-stress models. A third possibility is that the weakest-link assumption becomes increasingly invalid with increasing plasticity and micro-crack interaction effects need to be accounted for.

To improve the individual failure probability, the effect of the plastic strain has been introduced in modifications of the Beremin model [11, 12] as well as in incremental formulations [13]. Recently, in addition to plastic strains the effect of stress triaxiality has also been introduced [14]. In a previous work [15], we have compared these models with the original Beremin and demonstrated that they provide improvements in the predicted failure probability profiles ahead of cracks with different constraints. This comparison has been done against a large set of experimental data for the locations of cleavage initiation sites reported in [16]. However, the prediction of the cleavage fracture toughness temperature dependence with these models remained unsatisfactory when performed with single set of Weibull parameters calibrated at T_0. The effect of particle size on local failure probability was first proposed in [17]. The model now known as WST, however, remained as a microstructure-informed local model and to our knowledge had not been applied for global failure predictions. A different direction of work considers ductile damage prior to cleavage in the DBT regime, employing damage models for the material behaviour coupled with subsequent calculation of failure probability following Beremin [18, 19]. This approach has the potential to capture better the fracture behaviour in the DBT, but the models are presently too simplified with no interaction of void growth and micro-cracking at microstructure level [20]. Until advanced coupled models are developed and tested, the wider engineering community would benefit from a simpler uncoupled cleavage fracture model for the DBT region.

In [15] we have proposed a model incorporating mechanical and particle size effects and demonstrated that it provides excellent predictions for failure probability profiles. In this work we report on application of the model to predict cleavage fracture toughness in DBT regime. We focus on the first two possibilities mentioned above: to improve individual probability of failure and to account directly for the real particle size distribution rather than approximating the tail. The validity of the weakest-link assumption for the calculation of global probability is maintained. The model is applied to specific RPV steel, Euro Material A, for which fracture toughness data is available in [21] and particle size distribution, obtained via metallographic analyses, is given in [22].

2. Theory and model

LA methods share a common philosophy based on two distinct components. Firstly, the local mechanical fields provide a local or 'individual' probability of failure when linked to the size distribution of the micro-crack initiators. The individual probability of failure at location *i* is

$$p_{f,i} = \int_{r_{c,i}}^{\infty} p_{c,i}\ f(r)\, dr\,, \tag{2}$$

where *f(r)* is the probability density of initiators' sizes, $p_{c,i}$ is the probability of micro-crack nucleation, and $r_{c,i}$ is a critical micro-crack size at location *i*. Note, that $p_c\ f(r)$ is the probability density of nucleated micro-crack sizes. Existing LAs can be recast into Eq. (2) albeit with different definitions of p_c and r_c. For example in [2-4] $p_c = 0$ or 1 for zero and non-zero plastic strains. In [11, 12] p_c scales with the equivalent plastic strain, while in [14] p_c scales with the equivalent plastic strain and exponent of the stress triaxiality. In [13] p_c is a more complex function of stress and plastic strain increments. In all cases r_c is defined via Griffith or plasticity-modified Griffith criterion. Common feature of [2-4, 11-14] is that p_c is independent of particle size.

Secondly, it is assumed that the individual failure events are independent. This allows the weakest-link argument to be invoked for calculating the global failure probability, so that

$$P_f(V) = 1 - \prod_{i=1}^{N} \left(1 - p_{f,i}\right), \tag{3}$$

where *N* is the number of possible weakest-links, i.e. active micro-cracks, in volume *V*. In practice, LAs are applied to FE solutions of cracked components, where the mechanical fields are constant within an integration point volume, V_i. The failure probability of such a volume is thus

$$P_f(V_i) = 1 - \left(1 - p_{f,i}\right)^{N_i} = 1 - \left(1 - p_{f,i}\right)^{\rho_i V_i}, \tag{4}$$

where $N_i = \rho_i V_i$ is the number of micro-cracks in V_i, and ρ_i is the density of the micro-cracks. Strictly speaking $\rho_i = \rho\ p_{c,i}$, where ρ is the density of initiating particles in the material. The component probability of failure is then calculated by repeated application of (3) to get

$$P_f(V) = 1 - \prod_{i=1}^{IP} \left(1 - p_{f,i}\right)^{\rho_i V_i}\,, \tag{5}$$

where the product is taken over all integration points. When p_c is independent of particle size, Eq. (2) can have a closed-form solution in terms of critical micro-crack sizes, r_c. With a power law approximation for particle sizes and assuming small individual failure probabilities, Eq. (5) yields the Weibull-stress function in Eq. (1). We use Eq. (5) directly for global failure probability, because the experimental particle size distribution, Section 2.1, and our expression for individual failure probability, Section 2.3, do not allow for closed form solution of Eq. (2).

2.1. Experimental data

The material analysed is an RPV 22NiMoCr37 ferritic steel, known as Euro Material A, for which we have the mechanical and fracture toughness properties at a number of temperatures and irradiation states within the lower shelf and in DBT from the Euratom FP6 project PERFECT [21] and FP7 project PERFORM60. The temperature dependence of Young's modulus E, proportionality stress σ_0, and ultimate tensile strength σ_u under un-irradiated conditions are

$$E = -90T + 206000\,, \tag{6}$$

$$\sigma_0 = 421.2 + 63.9\exp\left(-T/91\right),\ \ \sigma_u = 564.1 + 70.2\exp\left(-T/108\right), \tag{7}$$

where T is in ^{o}C and E, σ_0, and σ_u are in MPa. Poisson's ratio is $\nu = 0.3$ independent of temperature. For the irradiated state considered here, fluence of 4.3 x 10^{19} n cm^{-2}, En > 1 MeV at 285ºC, E is given by Eq. (6) while σ_0 and σ_u are given by

$$\sigma_0 = 490.4 + 62.1\exp\left(-T/95.2\right),\ \ \sigma_u = 524.2 + 155.1\exp\left(-T/188.2\right). \tag{8}$$

The fracture toughness properties of Material A were determined according to the ASTM standard [23] using SEN(B) specimens in three-point bending [21]. This standard is based on the Master Curve formalism, which defines the temperature dependence of a reference toughness, K_0, relative to a reference temperature, T_0, at which K_0 = 108 MPa√m, for high-constraint cracked geometries with reference crack front length B_0 = 25.4 mm

$$K_0 = 31 + 77\exp\left[0.019\left(T - T_0\right)\right]. \tag{9}$$

The scatter in measured cleavage fracture toughness values is described as a function of the probability of failure, p, and the actual crack front length, B, with

$$K_p = K_{\min} + \left(K_0 - K_{\min}\right)\left(\frac{B_0}{B}\right)^{1/4}\left(\ln\frac{1}{1-p}\right)^{1/4}, \tag{10}$$

where $K_{\min}$ is a temperature independent threshold toughness, $K_{\min}$ = 20 MPa√m in [23]. Eqns. (9) and (10) define the cleavage fracture toughness behaviour of a material with known T_0. The reference temperatures for deep-notch (a_0/W = 0.5) specimens reported in [21] are T_0 = -104ºC for un-irradiated and T_0 = -78ºC for irradiated state. In the present work, we assume that Eqns. (9) and (10) provide a relevant representation of experimental data and assess our model against it.

The density and size distribution of cleavage initiating particles in Material A have been reported in [22]. The nature of the initiators has been determined by fractography revealing that cleavage in this material initiated predominantly at metal carbides, specifically M_3C and $M_{23}C_6$, and occasionally at carbide-sulphate composites. Comprehensive metallographic examination of carbides provided number density $\rho = 7.6\times10^{17}$ m^{-3} and a probability density of particle sizes which was fit by

$$f\left(r\right) = \frac{\beta}{r_0}\left(\frac{r}{r_0}\right)^{-\beta-1}\exp\left[-\left(\frac{r}{r_0}\right)^{-\beta}\right], \tag{11}$$

with shape $\beta = 2.7$ and scale r_0 = 0.036 μm.

2.2. Micro-mechanically informed model

The expression for the probability of particle failure is based on experimental observations that this probability depends not only on the mechanical fields but also on the particle size, similarly to the

WST model [17]. The rationale is that larger particles have higher probability of failure than smaller particles under identical mechanical conditions. The particles are assumed to be elastic-brittle with elastic constants equal to those of the matrix as a first approximation. The principle stresses, Σ_α, in a particle can be given in terms of the principal stresses, σ_α, and plastic strains, $\varepsilon^p{}_\alpha$, in the matrix with

$$\Sigma_\alpha = \sigma_\alpha + \frac{E}{1+\nu}\,\varepsilon_\alpha^p, \qquad \alpha = 1,2,3\,. \tag{12}$$

The criterion of particle failure is based on a critical value of the strain energy density in a particle associated with failure normal to the maximum principal stress. This is given by

$$\psi_c = \frac{1+\nu}{E}\,\Sigma_I^2 - \frac{\nu}{E}\,\Sigma_I\Sigma_h\,. \tag{13}$$

where Σ_I and Σ_h ($=\sigma_h$) are the maximum principal and the hydrostatic stress in the particle, respectively. If a particle of size r ruptures normally to the maximum principal stress upon achieving some critical condition, the energy lost (or the work of rupture) will be proportional to $\Psi_c = r^3 \cdot \psi_c$. The survival probability, p_s, of the particle must decrease with increasing work of rupture, which can be written in the form

$$\frac{dp_s}{p_s} = -\frac{d\Psi_c}{\Psi_0}\,, \tag{14}$$

where Ψ_0 is a scaling energy. The survival probability at a given Ψ_c can be determined by integrating Eq. (14) from the initial value of the work of rupture, which is zero, to the current value. The probability of particle rupture, p_c, is one minus the survival probability

$$p_c = 1 - \exp\left(-\frac{\Psi_c}{\Psi_0}\right) = 1 - \exp\left[-\left(\frac{r}{r_0}\right)^3 \frac{\psi_c}{\psi_0}\right], \tag{15}$$

where the rupture energy density scale $\psi_0 = \Psi_0 / r_0{}^3$ is introduced for convenience. Note, that Eq. (15) incorporates the effects of plastic strain and stress triaxiality. Increased plastic strains will result in increased ψ_c and hence probability of micro-crack formation. Inversely, increased hydrostatic stress, which could lead to micro-crack blunting, will result in reduced ψ_c and hence probability of micro-crack formation under equal other conditions, see Eqns. (12) and (13).

We use Eq. (15) and Eq. (11) into Eq. (2) to calculate individual probabilities of failure at the integration points by numerical integration. The lower limit of the integral, i.e. the critical micro-crack size, is defined with a heuristic argument leading to a new modification of the Griffith criterion. We assume that the behaviour of a micro-crack of radius r formed in the plastic matrix corresponds to a fictitious micro-crack with $r_f > r$ in an elastic matrix. The crack opening displacement of a penny-shaped crack of radius r_f in an elastic material subject to normal stress σ_I is

$$u(x) = \frac{4\left(1-\nu^2\right)\sigma_I}{\pi\, E}\sqrt{r_f^2 - x^2}\,, \qquad 0 < x < r_f\,. \tag{16}$$

The blunting of the physical micro-crack formed after particle rupture can be approximated by $r\varepsilon^p{}_I$. The fictitious micro-crack size is then defined in such a way that the opening at $x = r$ equals the blunting of the physical micro-crack, i.e. $u(r) = r\varepsilon^p{}_I$. Solving Eq. (16) with this constraint leads to the following expression for the fictitious micro-crack size

$$r_f = r\sqrt{1 + \left[\frac{\pi\, E\, \varepsilon_I^p}{4\left(1-\nu^2\right)\sigma_I}\right]^2}\,. \tag{17}$$

Used in conjunction with the Griffith criterion an effective critical micro-crack size can be defined

$$r_c = \frac{\pi E \gamma_s}{2\left(1-\nu^2\right)\sigma_I^2}\sqrt{1+\left[\frac{\pi E \varepsilon_I^p}{4\left(1-\nu^2\right)\sigma_I}\right]^2} \quad . \tag{18}$$

The square-root factor in Eq. (18) replaces the exponent of plastic strain in the modified Griffith criterion used previously [2-14]. As before, it is intended to account for the reduction in crack driving force due to plastic dissipation in the matrix. The difference is that in the case of Eq. (18) the effect is not only dependent on the plastic strain but also on stress triaxiality via the ratio between the maximum plastic strain and the maximum stress.

2.4. FE model

The developed LA has been applied to an FE model of Pre-Cracked Charpy-V (PCCV) specimens used in the tests [21]. These were 30 mm thick, 200 mm long and 25.4 mm deep. Here, this is modelled in 2D under plane strain conditions. Crack depth was 12.7 mm representing high constraint conditions. Rigid loading rollers were positioned with a total span of 180 mm (i.e. 10 mm from the specimen edge) and at the crack back-face. The FE model, with account for symmetry, was created and analysed with ABAQUS 6.11 [24]. The crack tip region was modelled as a fine blunt notch with a radius of 25 μm for use in large strain analyses. The crack tip elements were 5 μm long and 0.6 μm wide. In total 34,000 CPE8R elements were used. Model illustration is given in Fig. 1.

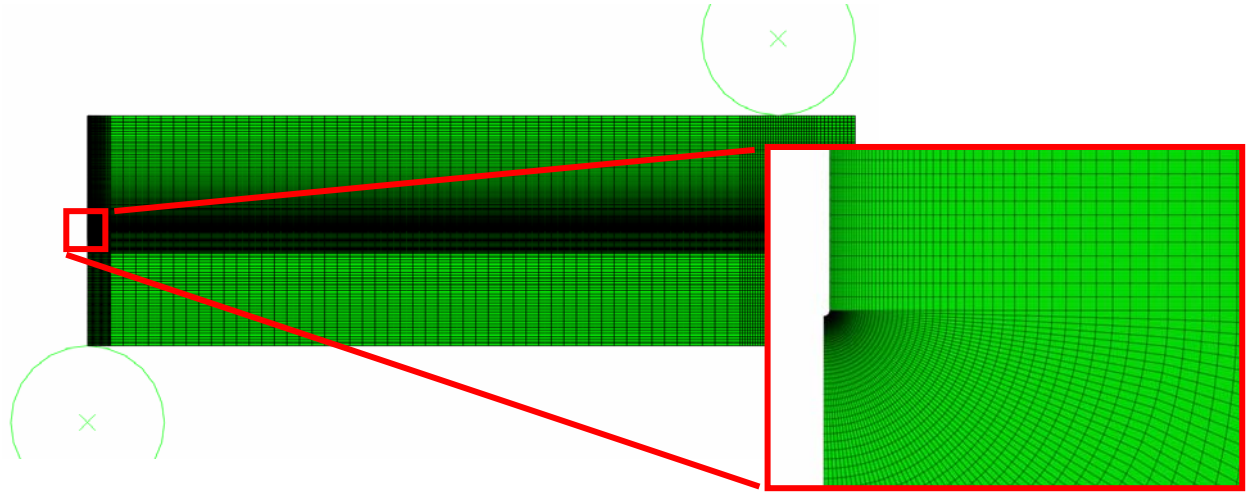

Figure 1. FE Model of 3PB specimen

We considered a range of temperatures in un-irradiated and irradiated states, spaced between approximately ±60°C of the un-irradiated T_0 in a maximum of 10°C increments. Power-law stress-strain relation was used to describe material behaviour at each temperature, such that $\varepsilon = \sigma/E$ for $\sigma < \sigma_0$, and $\varepsilon = (\sigma_0/E)(\sigma/\sigma_0)^n$ for $\sigma > \sigma_0$, where E was determined from Eq. (6) and σ_0 was determined from Eqns. (7) or (8). The power law exponent, n, was found using the Considère's rule describing the stress-strain condition at the point of loss of stability, represented by σ_u.

Loading was applied by displacing the bottom loading pin into the specimen whilst preventing the top pin from moving. It was also necessary to apply boundary conditions to the loading pins to prevent free rotation and unwanted displacement. Standard contact was used with a small adjustment of 0.015 mm to the mesh around the rigid surface of the loading pins to ensure correct transference of the load. The contact was also modelled as having no separation, ensuring contact throughout the analyses. Large strain analyses were performed in all cases.

In each analysis the *J*-contour integral, calculated by Abaqus, was used to determine the stress intensity factor for comparisons with Master Curve. The validity of *J* for this purpose can be questioned as the applied load caused the plastic zone to reach the back face and interact with the loading pin, preventing the contour zone from fully encompassing the plastic zone. To try and encompass as much of the plastic zone as possible up to 80 contours were taken away from the crack tip node set. Thus, the estimate of *J* covered as much of the plastic zone as possible whilst remaining contained in the model. Validation of the model was performed that provided confidence in the model, loading and extracted values of *J*.

3. Results and discussion

For known carbide distribution parameters, β and r_0, in principle the model requires a single calibration of the rupture energy density scale, ψ_0, in Eq. (15). This can be performed by comparing experimentally measured positions of cleavage initiation sites with the profile of the individual failure probability ahead of the crack, calculated using Eq. (2) with Eqns. (15) and (18). For surface energy γ_s = 2.4 Jm^{-2} available for typical ferritic steels in the literature [25] and β=2.7 we have previously calibrated ψ_0 using experimental data for Material A at several constraints and temperatures taken from [16] and found a value ψ_0 =10^5 that was fairly insensitive to such changes [15]. Here, we used this value for all cases analysed. However, to investigate the sensitivity of the results to variations in carbide size distribution we considered two shapes: the experimental β=2.7 and a higher β=4. To accommodate for this, keeping ψ_0 =10^5, we calibrated γ_s at a single temperature, T_0 for the un-irradiated material, so that at applied K = 100.3 MPa√m the model predicted 50% probability of cleavage. The calibrated values for γ_s were 2 Jm^{-2} for β=2.7 and 8 Jm^{-2} for β=4. Note that the calibrated γ_s for β=2.7 is within 20% to the literature value.

Fig. 2 shows two failure probability profiles as functions of normalised distance ahead of the crack obtained with β=2.7 and β=4 and the calibrated ψ_0 and γ_s. For both profiles r_0 = 0.036 μm is used. The green stars show experimentally measured locations of cleavage initiation sites reported in [16] for SEN(B) specimens with deep cracks tested to fracture at several temperatures. The results are normalised so that the maximum individual failure probability is at unity. Note that the predicted profiles do not change significantly with the shape β, suggesting a small dependence of the calibration results on particle size distribution. Clearly, the model captures the peak location of initiating particles accurately and approximates the overall shape sufficiently well. The experimental β=2.7 appears to give a slightly better fit.

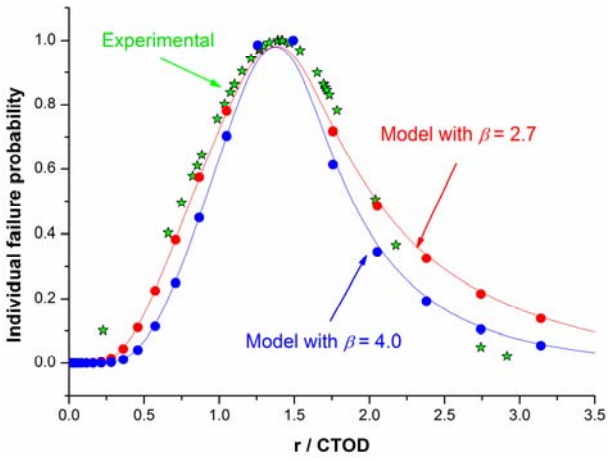

Figure 2. Individual failure probability predicted by proposed model with β = 2.7 and β = 4.

The predictive bounds from the model compared to both experimental data and the Master Curve are given in Fig. 3 for the un-irradiated material for both the β=2.7 (left) and β=4 (right) carbide size distributions. It can be seen that our model provides a good fit of the experimental data for both values of β with only a couple of points slightly outside the lower bound prediction. This, however, is also observed for the Master Curve. The comparison to the Master Curve is very good over the lower transition region before becoming slightly wider at higher temperatures. This provides confidence in the finite element analyses and developed local approach model. That the results widen at higher temperatures is likely to be an effect of plasticity which could manifest in both the accuracy of the finite element analyses and of the assumptions in the local approach model. The effect of changing β is only slight over the lower DBT transition region, where the higher value of β provides a narrower probability bound, as reflected in Fig. 2.

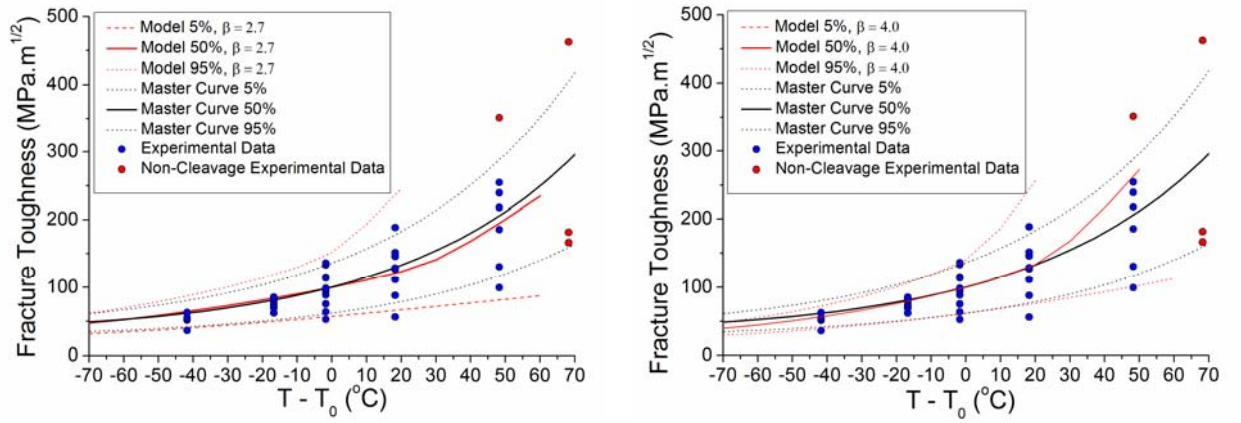

Figure 3. Temperature dependence predicted by proposed model with β = 2.7 (left) and β = 4.0 (right) for the un-irradiated material. Experimental data and Master Curve predictions shown for comparison.

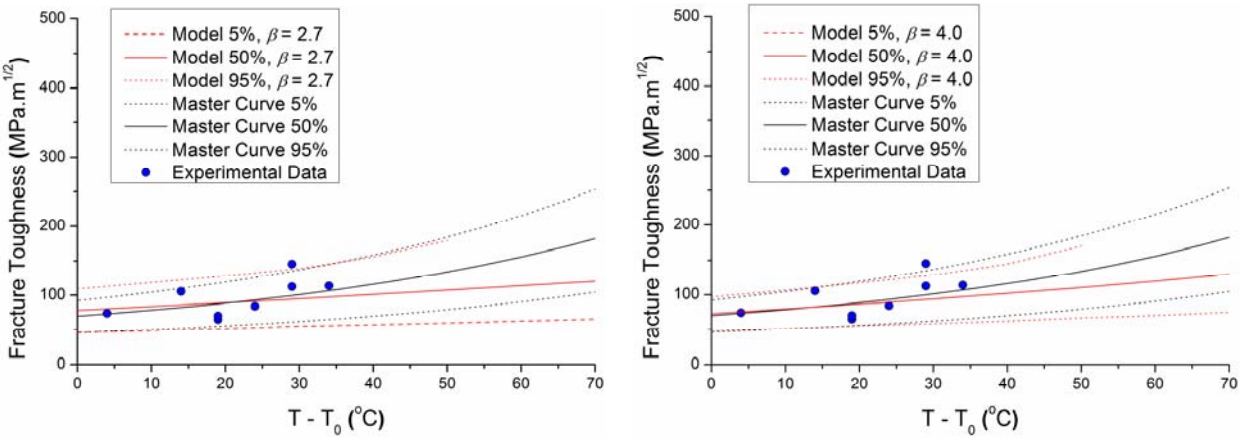

Figure 4. Temperature dependence predicted by proposed model with β = 2.7 (left) and β = 4.0 (right) for the irradiated material (4.3 x 10^{19} n cm^{-2}, En > 1 MeV at 285°C).

The predictive bounds from the model for the irradiated material are given in Fig. 4, again with β =2.7 (left) and β =4 (right) carbide size distributions. It can be seen that both the developed model and the Master Curve profiles provide a good fit to the experimental data. It must be emphasised that our model's predictions are based only on the changes in the tensile properties from the un-irradiated analyses while the calibrated model parameters were the same. At the same time the position of the Master Curve is dictated by the experimentally determined T_0 for the irradiated state.

If assessed in terms of a shift in the Master Curve T_0 value the proposed model provides a +33°C reference temperature shift, whereas the Master Curve assessment provides a +29°C shift. This means that the model has, for this case, accurately predicted the shift in toughness with irradiation with some additional safety margin.

The strong side of the proposed model is that it offers a microstructure-property relation that remains as true to the physics as presently possible within the constraints of the uncoupled material behaviour and the weakest-link assumption. The model takes directly microstructure data: the density of initiators and the probability distribution of their sizes, which can be determined by metallography. It basically requires the calibration of a single parameter: the rupture energy density scale, for which the additional information for positions of cleavage initiators can be determined by fractography. In the particular case reported here, the surface energy was also calibrated. This however was necessary to study a distribution with a higher than the experimental shape, while the scale parameter and density of initiators remained the same. It should be noted that the shape, scale and density are intrinsically related for a given material, so that the need to calibrate the surface energy could be eliminated for accurate experimental data. We have shown, at least in principle, that by advancing the local failure probability expression and accounting for a "real" size distribution data, one can achieve improved predictions for cleavage fracture toughness, certainly in the lower transition region. The outcome at higher temperatures is not yet satisfactory, but the reason for this could be the third possibility described in the introduction: interactions between micro-cracks, the density of which increases with plasticity, may become strong enough to invalidate the weakest-link assumption behind the current model. This will be a subject of future investigations.

4. Conclusions

- The proposal offers a microstructure-informed strategy for calculating the probability of failure in a large part of the DBT region.
- The calibration provides an estimate of surface energy that is close to values available in the literature, indicating that if all available parameters were well defined, the model would provide meaningful predictions of fracture toughness.
- The predicted initiation sites (individual probability profiles) correspond very well with experimentally determined initiation sites for this material.
- Cleavage toughness predictions in the DBT regime correlate well with both experimental data and Master Curve fits in the un-irradiated state.
- On changing the tensile properties to consider irradiation, the shift in fracture toughness and spread of experimental results are well predicted. This is achieved with a single calibration at one temperature in the unirradiated state.

Acknowledgements

The support from BNFL to Jivkov is gratefully acknowledged. James would also like to acknowledge assistance from colleagues at AMEC in the FEA and to PERFORM60 for data.

References

[1] A. Pineau, Development of the local approach to fracture over the past 25 years: theory and applications. Int J Fract 138 (2006) 139–166.
[2] F.M. Beremin, A local criterion for cleavage fracture of a nuclear pressure vessel steel. Metal Trans 14A (1983) 2277-2287.
[3] F. Mudry, A local approach to cleavage fracture. Nucl Eng Design 105 (1987) 65-76.

[4] F. Minami, A. Bruckner-Foit, D. Munz, B. Trolldenier, Estimation procedure for the Weibuli parameters used in the local approach. Int J Fract 54 (1992) 197-210.
[5] C. Ruggieri, R.H. Dodds Jr., A transferability model for brittle fracture including constraint and ductile tearing effects: a probabilistic approach. Int J Fract 79 (1996) 309-340.
[6] X. Gao, R.H. Dodds Jr., Constraint effects on the ductile-to-brittle transition temperature of ferritic steels: a Weibull stress model. Int J Fract 102 (2000) 43–69.
[7] J.P. Petti, R.H. Dodds Jr., Calibration of the Weibull stress scale parameter, σ_u, using the Master Curve. Eng Fract Mech 72 (2005) 91–120.
[8] B. Wasiluk, J.P. Petti, R.H. Dodds Jr., Temperature dependence of Weibull stress parameters: Studies using the Euro-material. Eng Fract Mech 73 (2006) 1046–1069.
[9] P. Akbarzadeh, S. Hadidi-Moud, A.M. Goudarzi, Global equations for Weibull parameters in a ductile-to-brittle transition regime. Nucl Eng Design 239 (2009) 1186–1192.
[10] Y. Cao, H. Hui, G. Wang, F.-Z. Xuan, Inferring the temperature dependence of Beremin cleavage model parameters from the Master Curve. Nucl Eng Design 241 (2011) 39-45.
[11] G. Xiaosheng, G. Zhang, T.S. Srivatsan, A probabilities model for prediction of cleavage fracture in the ductile-to-brittle transition region and the effect of temperature on model parameters. Mater Sci Eng 415A (2006) 264-272.
[12] M. Kroon, J. Faleskog, H. Oberg, A probabilistic model for cleavage fracture with a length scale – Parameter estimation and predictions of growing crack experiments. Eng Fract Mech 75 (2008) 2398-2417.
[13] S.R. Bordet, A.D. Karstensen, D.M. Knowles, C.S. Wiesner, A new statistical local criterion for cleavage fracture of steel. Part I: model presentation. Eng Fract Mech 72 (2005) 435-452.
[14] J. Hohe, V. Hardenacke, S. Luckow, D. Siegele, An enhanced probabilistic model for cleavage fracture assessment accounting for local constraint effects. Eng Fract Mech 77 (2010) 3573-3591.
[15] A.P. Jivkov, D.P.G. Lidbury, P. James, Assessment of local approach methods for predicting end-of-life toughness of RPV steels. In Proc PVP2011 (2011) paper 57546, Baltimore, USA.
[16] J. Hohe, V. Friedmann, J. Wenck, D. Siegele, Assessment of the role of micro defect nucleation in probabilistic modeling of cleavage fracture, Eng Fract Mech 75 (2008) 3306–3327.
[17] K. Wallin, T. Saario, K. Torronen, Statistical model for carbide induced brittle fracture in steel. Metals Sci 18 (1984) 13-16.
[18] L.C.A. Folch, F.M. Burdekin, Application of coupled brittle-ductile model to study correlation between Charpy energy and fracture toughness values. Eng Fract Mech 63 (1999) 57-80.
[19] G. Bernauer, W. Brocks, W. Schmitt, Modifications of the Beremin model for cleavage fracture in the transition region of a ferritic steel. Eng Fract Mech 64 (1999) 305-325.
[20] A. Pineau, Modeling ductile to brittle fracture transition in steels - micromechanical and physical challenges. Int J Fract 150 (2008) 129–156.
[21] E. Keim, Summary of material data for 22NiMoCr37. Areva ANP GmbH, Technical Report, 2005.
[22] S.R. Ortner, J. Duff, Characterisation of Euro 'A' reference steel for application of EOH model of brittle fracture. Nexia Solutions, Technical Report, 2005.
[23] ASTM E 1921-05, Standard Test Method for Determination of Reference Temperature T_0 for Ferritic Steels in the Transition Range. ASTM, 2005.
[24] ABAQUS 6.11, DS Simulia Corp, 2011.
[25] A. Hung, I. Yarovsky, J. Muscat, S. Russo, I. Snook, R.O. Watts, First-principles study of metallic iron interfaces. Surface Sci 501 (2002) 261-269.